ACS APPLIED MATERIALS & INTERFACES

Research Article

www.acsami.org

Rheology and Morphology of Pristine Graphene/Polyacrylamide Gels

Sriya Das, Fahmida Irin, Lan Ma, Sanjoy K. Bhattacharia, Ronald C. Hedden, and Micah J. Green*

Department of Chemical Engineering, Texas Tech University, Lubbock, Texas 79409, United States

Supporting Information

ABSTRACT: Enhancement of toughness in nanomaterial-based hydrogels is a critical metric for many of their engineering applications. Pristine graphene-polyacrylamide (PAM) hydrogels are synthesized via in situ polymerization of acrylamide monomer in PAM-stabilized graphene dispersion. In-situ polymerization leads to the uniform dispersion of the graphene sheets in the hydrogel. The graphene sheets interact with the elastic chains of the hydrogel through physisorption and permit gelation in the absence of any chemical cross-linker. This study represents the first report of pristine graphene as a physical cross-linker in a hydrogel. The properties of the graphene-polymer hydrogel are characterized by rheological measurements and compressive tests, revealing an increase in the storage modulus and toughness of the hydrogels compared to the chemically cross-linked PAM analogues. The physically cross-linked graphene hydrogels also exhibit self-healing properties. These hydrogels prove to be efficient precursors for graphene-PAM aerogels with enhanced electrical conductivity and thermal stability.

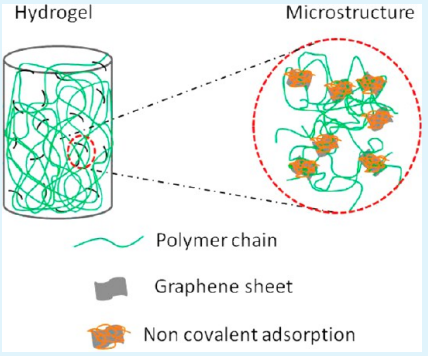

KEYWORDS: *pristine graphene, polymer, hydrogel, rheology, modulus, aerogel*

1. INTRODUCTION

Hydrogels are three-dimensional networks of cross-linked polymer chains swollen with water. Cross-linking of the network may be accomplished via chemical (covalent bonds) or physical (ionic interactions, microcrystallites, or hydrogen bonding) means. Hydrogels have a wide array of applications, including actuators, biosensors, sustained drug-release, and drug delivery systems.[1−4] However, as the mechanical properties (toughness, crack resistance) of the hydrogels are often poor, it limits the performance of the gels in some applications. Tough and highly ductile gels have been fabricated in the past using the concept of tetrahedron-like macromonomers and double networks.[5−7] The addition of nanofillers such as silica, clay, and carbon nanotubes has also been used to enhance the hydrogel mechanical strength and toughness.[8−14]

In this paper, we focus on graphene as reinforcing nanofiller in polyacrylamide hydrogels, with an emphasis on pristine (unfunctionalized) graphene. Graphene, that is, one-atomic-layer thick sheets of sp^2 hybridized carbon atoms, is well-known for its outstanding electrical, mechanical, and thermal properties.[15] The term "pristine" is mainly used to distinguish these graphene sheets from those that have been processed through covalent functionalization.[15−18] However, dispersing graphene in polymer or solvents is a challenge because of restacking and aggregation of the sheets, which is caused by the strong intersheet van der Waals forces. The preparation of dispersed graphene via the graphite oxide route is the most common technique for the liquid phase processing of graphene. There are two general steps involved in this method: (1) oxidation of parent graphite to yield graphene oxide (GO), and (2) the reduction of GO sheets in presence of stabilizers to produce reduced graphene oxide (RGO).[19,20] However, GO sheets are electrically insulating, and the unique properties of pristine graphene are only partially restored after reduction.[21] Recent studies have also suggested the presence of anomalous oxidative debris associated with colloidal GO.[22]

Given these difficulties, we choose the pristine graphene route in the current work. In this procedure, the parent graphite is sonicated in the presence of stabilizers such as surfactants, polymers, or aromatic $\pi-\pi$ stacking molecules.[18,23−28] These molecules noncovalently adsorb onto or wrap around the graphene surface and prevent reaggregation of the graphene sheets, leading to stable dispersions of pristine graphene in the desired solvent. Prior literature also demonstrates that this technique yields pristine, almost defect-free graphene. These techniques can easily yield high-concentration dispersions of pristine graphene in water (~0.6−0.8 mg/mL).[25,28,29]

There are a number of recent reports on GO based hydrogels. Liu et al. have successfully fabricated graphene-oxide-polyacrylamide (PAM) hydrogels via hydrogen bonding of the GO surface with the PAM chains.[30] The nanocomposite hydrogels of GO and polymer also exhibit self-healing properties.[31−33] Shen et al. have fabricated GO-PAM chemically cross-linked hydrogels with increased mechanical strength.[34] A number of recent reports have focused on the use of GO in hydrogels. GO-based hydrogels are of special interest because of their ability to form self-assembled structures in the presence of a physical cross-linker.[31,35−39] GO and RGO sheets have also been used as physical cross-linkers, thus eliminating the need for chemical cross-linking

Received: June 5, 2013
Accepted: August 5, 2013
Published: August 5, 2013

   dx.doi.org/10.1021/am402185r | ACS Appl. Mater. Interfaces 2013, 5, 8633−8640

agents.[30,34,40] Fan et al. have utilized pristine graphene flakes to enhance the toughness of chemically cross-linked polyacylic acid (PAA) hydrogels.[41] Hence, this is indeed the first report of pristine graphene as a physical cross-linker.

In this work, we demonstrate the preparation of pristine graphene-PAM hydrogels. The graphene-PAM hydrogels are fabricated via in situ polymerization of the monomers in the graphene dispersion. The presence of the graphene enhances the shear modulus of the chemically cross-linked PAM hydrogels. We also successfully fabricate physically cross-linked graphene-PAM hydrogels. The graphene sheets act as effective cross-link junctions and can produce gelation in the absence of any chemical cross-linking agent. Compressive tests reveal that the incorporation of graphene lead to tougher hydrogels compared to the analogous chemically cross-linked PAM hydrogels. These graphene-PAM hydrogels exhibit unique self-healing properties. Finally, the graphene-PAM hydrogels are subsequently freeze-dried to yield graphene-polymer aerogels with increased thermal stability and electrical conductivity.

2. EXPERIMENTAL METHODS

Materials. Expanded graphite was provided by Asbury Carbons (CAS# 7782-42-5, grade 3805). The stabilizer, PAM with nominal molar mass of 5×10^6 g/mol (nonionic water-soluble), acrylamide (AM, monomer, ≥99% HPLC grade), *N,N*-methylenebisacrylamide (MBA, chemical cross-linker, 99%), and potassium persulfate (KPS, redox initiator, 99.99%, trace metal basis) were purchased from Sigma Aldrich. All the purchased chemicals were used as received.

Preparation of Graphene Dispersion. PAM powder (10 mg/mL) was added to deionized water (DI) and magnetically stirred for 48 h to obtain a clear solution. Expanded graphite (50 mg/mL) was then added to this PAM solution and tip sonicated at 8 W power using a Misonix sonicator (XL 2000) for 90 min at room temperature. The dispersion was then centrifuged (Centrific Centrifuge 225, Fischer Scientific) at ∼5000 rpm for 4 h to remove larger aggregates. The supernatant was collected for dispersion characterization and preparation of the graphene-PAM hydrogels.

Preparation of Graphene Hydrogels. A series of chemically cross-linked pure polyacrylamide (PAM) gels and graphene-loaded chemically cross-linked and physically cross-linked PAM gels were synthesized. Pure PAM hydrogels were synthesized using acrylamide, *N,N*-methylenebisacrylamide (MBA), and potassium persulfate ($K_2S_2O_8$). AM was initially dissolved in DI water (100 mg/mL). MBA (16 mg/mL) and $K_2S_2O_8$ (75 mg/mL) solutions were then added to the monomer solution.[42] The precursor solution was polymerized at 70 °C. In both the pure and the nanocomposite hydrogels, the same concentration of PAM was maintained. In the case of the chemically cross-linked graphene-PAM hydrogels, all the reactants were added to the graphene dispersion in water. However, for the physically cross-linked gels, MBA, chemical cross-linker was omitted. The graphene content values reported are based on the calculated mass of the polymer hydrogels (excluding water). The gels were stored in an aqueous environment at room temperature.

Dispersion Characterization. The graphene concentration of the supernatant of the centrifuged PAM-stabilized graphene dispersion was determined by absorbance measurements.[18] To measure the graphene concentration of the dispersions, the samples were filtered through PTFE filters (Millipore, 0.2 μm), dried overnight at 40 °C and the change of mass of the filter paper was estimated. The filter paper weighed 0.06 g and the graphene weighed ∼0.002 g (5 mL of 0.4 mg/mL dispersion). The measuring balance is sensitive up to 0.1 mg. For a PAM concentration of 10 mg/mL the graphene concentration was found to be 0.4 mg/mL in water. To correlate concentration with absorbance, UV−vis spectroscopy was performed on a Shimadzu UV−vis spectrophotometer 2550 at a wavelength range of 200 to 800 nm. To eliminate the background effect, that is, the effects of the polymer solution, the absorbance was measured against the PAM solution without graphene.

Transmission electron microscopy (HRTEM) was performed on the PAM-stabilized graphene dispersion. HRTEM samples were prepared by drop coating 20 μL of dispersion onto holey carbon grids (Electron Microscopy Sciences, HC200-Cu) and air-driying for 1 min. A Hitachi H8100 HRTEM with a voltage of 75 kV was used to image the specimens.

Hydrogel Characterization. Oscillatory shear measurements were performed on the as-prepared hydrogels. An Anton Paar strain-controlled rheometer (MCR 301) was used with parallel plate geometry (25 mm diameter). A gap of 2 mm was maintained during the course of the measurement. To determine a linear viscoelastic regime, the storage and loss moduli were monitored by varying strain% from 0.001% to 100% at a frequency of $\omega = 1\ s^{-1}$. Dynamic frequency sweeps from $\omega = 0.1$ to 100 s^{-1} were performed on each sample to determine the storage and loss moduli (G' and G''). The experiments were conducted in isothermal conditions of 25 °C.

Swelling experiments were performed on preweighed, cut samples of the hydrogels. The samples were immersed in a 1000X volume of distilled water (pH = 7.1) after curing and swelled to equilibrium (at least 5 days) at 23 °C. The gels were placed into fresh distilled water beakers, and the water was changed regularly to ensure proper extraction of solubles. The equilibrium mass swelling ratio (Q_s) was calculated according to eq 1:

$$Q_s = \left(\frac{M_s - M_{ex}}{\rho_1}\right)\left(\frac{\rho_2}{M_{ex}}\right) + 1 \quad (1)$$

In eq 1, M_s is the total mass of the hydrogel at equilibrium swelling, M_{ex} is the mass of the extracted gel after drying, and ρ_1 and ρ_2 are the densities of water and PAM in dissolved state, respectively. To obtain the M_{ex}, the samples were dried at room temperature for 2 d and then subsequently dried in a vacuum oven for 3 d at 40 °C.

Compressive tests were performed on hydrogels at 25 °C with a TA Q800 dynamic mechanical analyzer. Cylindrical disks of gels with a diameter of 2 cm and an initial thickness of 2 mm were molded. Gel disks were placed in between two parallel metal plates (fixture diameter = 4 cm) and a controlled force experiment was conducted on each gel. The samples were preloaded to a force of 0.05 N, followed by ramping the force linearly to 15 N at the rate of 0.005 N/min. Stress−strain data obtained from the dynamic mechanical analysis were utilized to compute the elastic modulus of each gel.

Aerogel Characterization. The pure and graphene-containing hydrogels were flash frozen in liquid nitrogen and then dried in a freeze-drier (Vitris Benchtop Freeze-Dryer) overnight to yield dry aerogel samples. The morphology of the fracture surface of the dried hydrogels was observed in a HITACHI S4300 electron microscope at an accelerating voltage of 5 kV. SEM samples were prepared by sputter coating with Au/Pd in Hummer V Technics sputter coater at 10 kV and 10 mA current for 1.5 min at a rate of 10 nm/min.

Electrical resistivity of the freeze-dried hydrogels (aerogels) was measured by the standard four point probe method. The four point probe head (Signatone, SP4−40045TBY) was mounted on a resistivity measurement stand (Signatone, Model 302). The probe head consists of four equally spaced tungsten tips, and the spacing between two tips is ∼1 mm. To minimize sample damage during probing each tip was supported by springs. Two outer probes were connected to a high impedance current source (Keithley 2400) to supply current through the sample and inner probes were coupled with a digital voltmeter (Keithley 2000) to measure the voltage drop across the two probes. Electrical resistivity and conductivity of the samples were determined from the applied current and measured voltage drop.

Thermogravimetric analysis was performed in a Metler Toledo (TGA/SDTA 851e, made in Switzerland) instrument to determine the thermal stability of the composites. Samples (∼15 mg) were heated from room temperature to 450 °C at a rate of 10 °C/min in a nitrogen atmosphere. The degradation temperatures were obtained from the differential TGA curves.

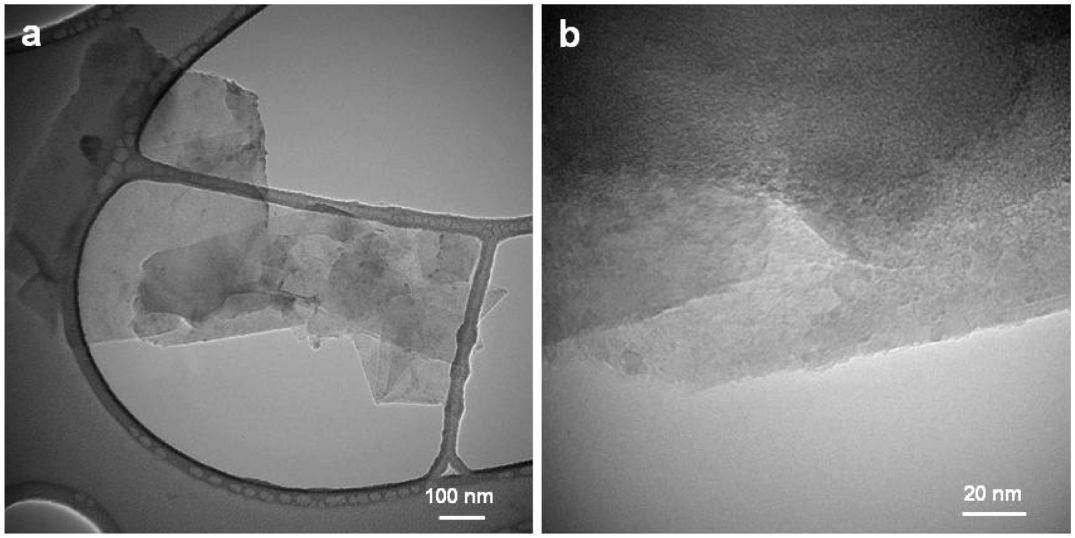

Figure 1. HRTEM images of (a) PAM-stabilized graphene and (b) magnified edge view of the same graphene sheet. The edge count indicates that the graphene is 3−5 layers thick.

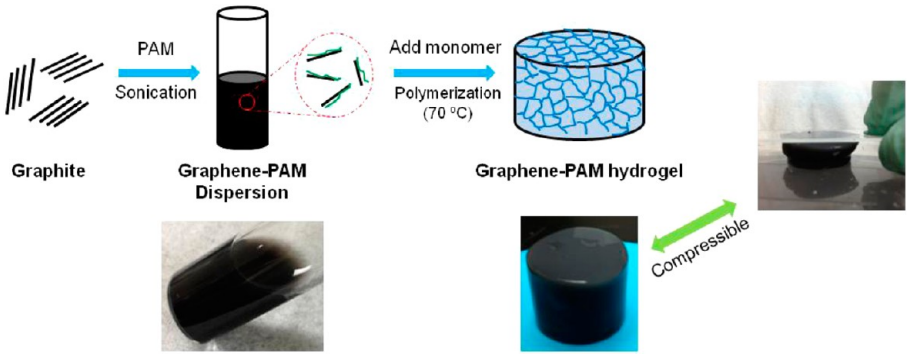

Figure 2. Schematic of sample preparation protocol by PAM followed by in situ polymerization to yield compressible graphene-PAM hydrogels.

3. RESULTS AND DISCUSSION

Hydrogel Microstructure. The uniform dispersion of graphene sheets in the hydrogel requires proper exfoliation of graphene in water. Several previous reports, including our own work, illustrate the use of water-soluble polymer such as polyvinylpyrrolidone (PVP) and PAM as stabilizers for aqueous graphene dispersions.[23,27,40] This technique of preparing a graphene dispersion with PAM as a stabilizer was previously demonstrated by Ren et al.[40] PAM was found to be physisorbed on the graphene surface, and the AFM images on the sample confirmed that the graphene sheets were individually dispersed in water with a thickness of ∼4.5 nm (the thickness of the polymer layer was 3 nm). In our study, we stabilized graphene with both high (5×10^6 g/mol) and low (10,000 g/mol) molar mass PAM chains. The data indicate that the former is more efficient in stabilizing graphene (Supporting Information, Figure S1), so the high molar mass PAM was used for the duration of the study. The absorbance spectrum of the PAM-stabilized graphene dispersion is shown in the Supporting Information, Figure S2a.

High resolution TEM is commonly used to characterize the thickness of colloidal graphene sheets.[18,23,29] The images of the dispersion show that the PAM chains successfully stabilized few-layer graphene sheets in water, which is in agreement with earlier studies (Figure 1).[23,25,28] The edge count in Figure 1b confirms that the PAM-stabilized graphene was indeed 3−5 layers thick. The sample preparation technique for the imaging is likely to induce aggregation; however, no graphene aggregates were observed. Additional HRTEM images depict the aspect ratio of the graphene sheets (Supporting Information, Figure S3), which is estimated at 100−400 based on the observation of 15 grids.

The graphene-PAM hydrogel was prepared by adding the monomer (acrylamide), the chemical cross-linker (MBA), and the initiator ($K_2S_2O_8$) to the graphene-PAM dispersion and conducting in situ polymerization. Figure 2 schematically depicts the preparation protocol for the graphene-PAM hydrogels. These hydrogels were subsequently characterized to quantify the effect of graphene sheets on mechanical properties of the network.

The graphene-PAM hydrogels were synthesized in both the absence and the presence of chemical cross-linkers. The formation of the graphene-PAM hydrogels in the absence of a chemical cross-linker was particularly intriguing. (PAM-only hydrogels must be synthesized using a chemical cross-linker.) There are several instances of nanoparticles such as clay, and multiwalled carbon nanotubes acting as physical cross-linkers;[12,30,43] however, utilizing pristine graphene sheets as a physical cross-linkers in hydrogels is novel. We propose that the PAM chains entangle with the PAM-stabilized graphene sheets through physisorption and noncovalent absorption and lead to the formation of the network (Figure 3). These graphene-PAM

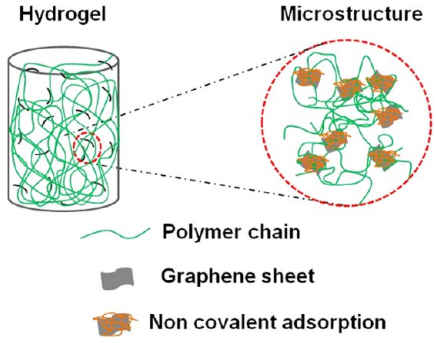

Figure 3. Proposed structure of the physically cross-linked graphene-PAM hydrogels.

physical hydrogels are different from the GO-loaded PAM hydrogels, in which hydrogen and ionic bonding on oxygen-containing sites of the GO sheets aid in the hydrogel formation.[30]

Frequency-dependent oscillatory shear experiments were applied to characterize the viscoelastic properties of all samples (Figure 4). Strain-dependent oscillatory shear experiments were initially performed to determine the limit for linear viscoelastic behavior, which showed an onset of nonlinearity at γ = 0.1% (Supporting Information, Figure S4). All subsequent dynamic measurements were carried out at 0.05% strain. The mechanical spectra showing the storage modulus (G') and the loss modulus (G'') as a function of the angular frequency (ω) are utilized to characterize the microstructure of the hydrogels. The effects of the monomer concentration, initiator type, and temperature on the PAM hydrogel are discussed in the Supporting Information, Figure S5. Increasing the graphene content increases the storage modulus of the nanocomposite hydrogels (Figure 4b). It is observed that for the chemically cross-linked gels, $G' \sim \varphi^{1.05}$ and for the physically cross-linked gels, $G' \sim \varphi^{0.88}$. These values are close to the exponential factor predicted for colloidal silica gels.[44] The marked increase in G' with graphene loading in the physically cross-linked network indicates the existence of strong interactions between the stabilized-graphene sheets and the PAM chains. This interaction leads to an enhancement of the elastic modulus of the graphene-loaded hydrogels.[13,45−50] Similar conclusions were drawn in the past for nanoparticle-loaded hydrogels in which strong interactions between polymer and nanoparticles exist.[8,12,48−50]

Few prior studies have actually quantified the effect of nanofillers on the effective concentration of elastic chains (N^*) in a gel at the measured frequency.[8,47] N^* includes the effects of

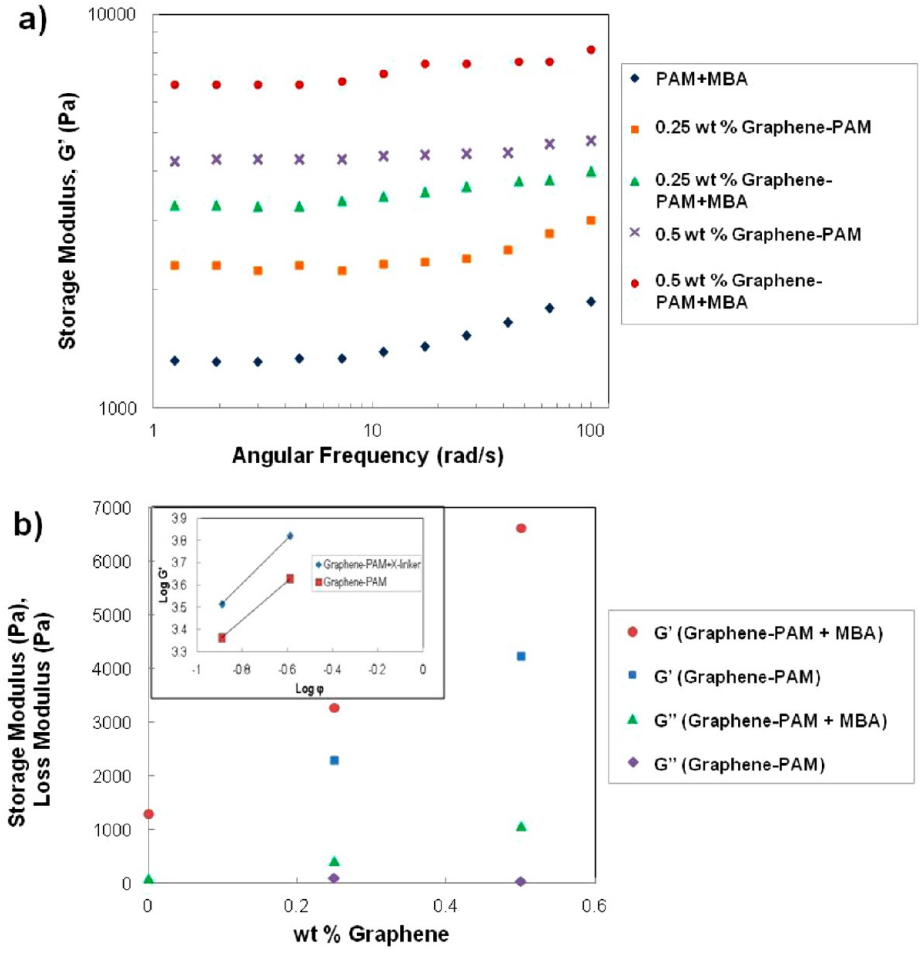

Figure 4. (a) Frequency-dependent storage moduli of the pure and nanocomposite hydrogels with varying graphene loadings. (b) Equilibrium storage modulus increases with increasing graphene content. The inset figure shows the scaling of the storage modulus with the vol % of graphene loading in the hydrogels. These results confirm that the physical interaction between polymer chains and graphene sheets leads to the enhancement of the modulus.

both covalent linkages and physical entanglements. The presence of the nanofiller affects N^* and can be analyzed based on rubber elasticity theory, which states that N^* (mol/m^3) is related to the equilibrium shear modulus, G_e of the hydrogel according to eq 2[51]

$$G_e = N^*RT \quad (2)$$

This analysis assumes affine deformation of elastic chains. As graphene content increases, the effective concentration of elastic chains increases (Figure 5). It is also observed that the

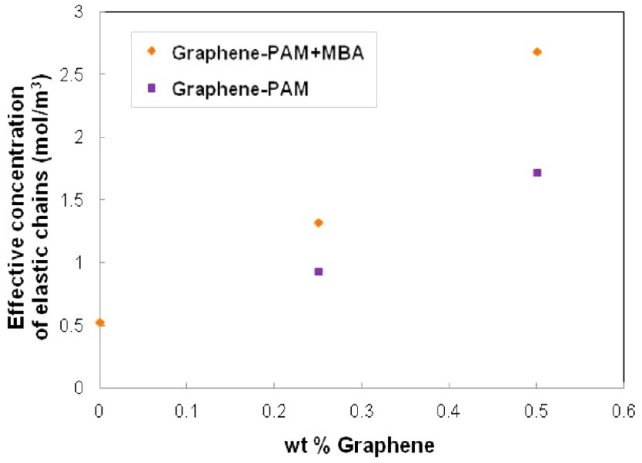

Figure 5. Variation in effective concentration of elastic chains of the nanocomposite hydrogel matrix. With increasing graphene content in the cross-linked network, the effective concentration of chains increases.

N^* values are lower for the physically cross-linked hydrogel than the chemically cross-linked hydrogel. Thus, the effective concentration of the elastic chains is lower in the physical gels, imparting a higher degree of mobility to the surrounding polymer network strands.

Swelling data are shown in Figure 6. The equilibrium mass swelling ratio decreases with increasing graphene content for both the physically and chemically cross-linked gels. The swelling properties of hydrogels mainly depend on the effective concentration of the elastic chains of the hydrogels. Again, the decrease in degree of swelling with the increase in graphene loading substantiates the notion that the graphene sheets act as cross-linking points. Similar results have been reported in the past for other nanofiller-loaded hydrogels;[8,12,34,52] however, this study is the first evidence of physically cross-linked gels withstanding swelling forces (Figure 6b). Note that the physical gels (graphene cross-linked) had a higher swelling ratio compared to the chemically cross-linked gels and swelled to equilibrium without dissolving. These remarkable results confirm that the physisorption of the PAM chains on the surface of graphene is strong enough to prevent disruption by solvent (water).

Compressive tests were conducted on the pure PAM hydrogel and the physically cross-linked graphene-PAM hydrogels. Figure 7a shows that as graphene content increases, the elastic modulus of the cross-linked network increases (Figure 7b). This observation confirms that the graphene sheets act as effective physical cross-linking points and provides greater stiffness modulus compared to pure PAM hydrogels (chemically cross-linked network). It is also observed that with the increase in graphene loading, the toughness of the hydrogel

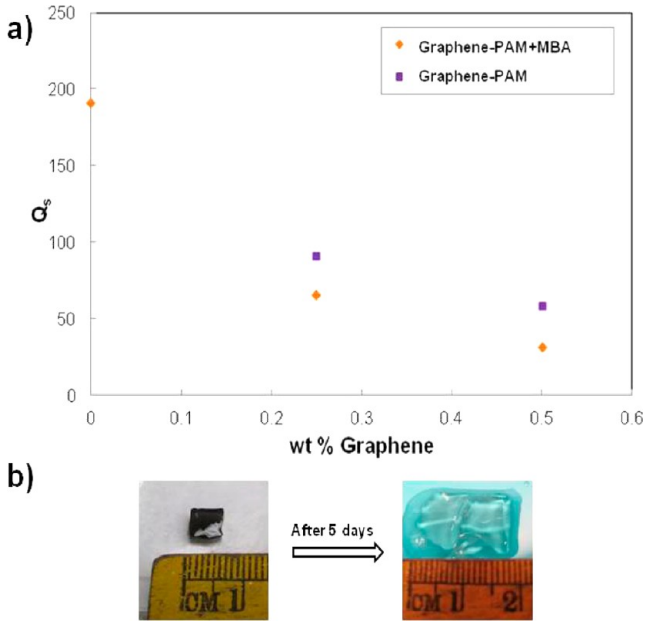

Figure 6. Equilibrium swelling ratio of the graphene-loaded hydrogels in water. The swelling ratio of the physically cross-linked hydrogels is higher than that of the chemically cross-linked gels.

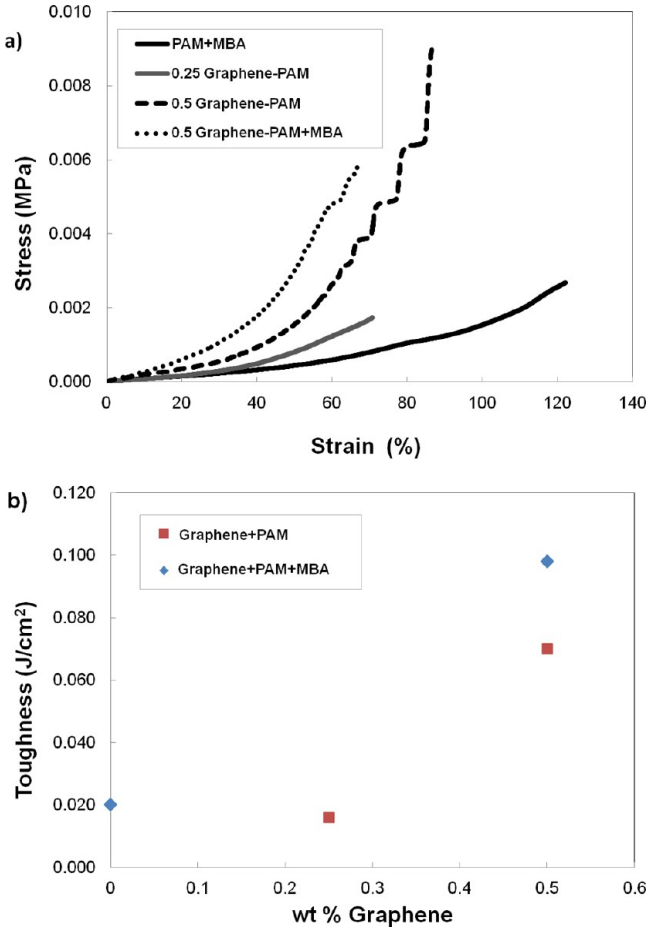

Figure 7. (a) Compressive stress-stain plots and (b) Toughness of PAM hydrogels with varying graphene content. This observation confirms that the graphene sheets act as effective physical cross-linkers and the network structure of the physical hydrogels is comparable to the chemically cross-linked graphene-PAM hydrogels.

dx.doi.org/10.1021/am402185r | ACS Appl. Mater. Interfaces 2013, 5, 8633−8640

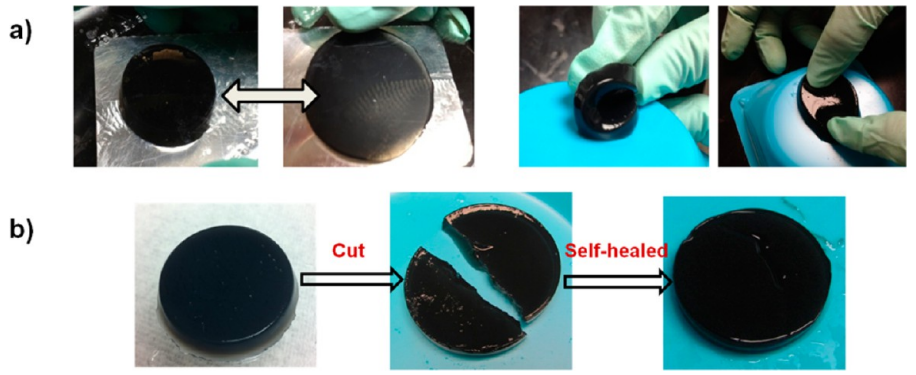

Figure 8. Physically cross-linked gels (a) could be compressed with a glass slide, freely bent and greatly extended. (Note that the mark resembling a fingerprint in the second picture of (a) is on the metal surface. As the sample is compressed, it becomes translucent making the mark visible), and (b) exhibits self-healing property.

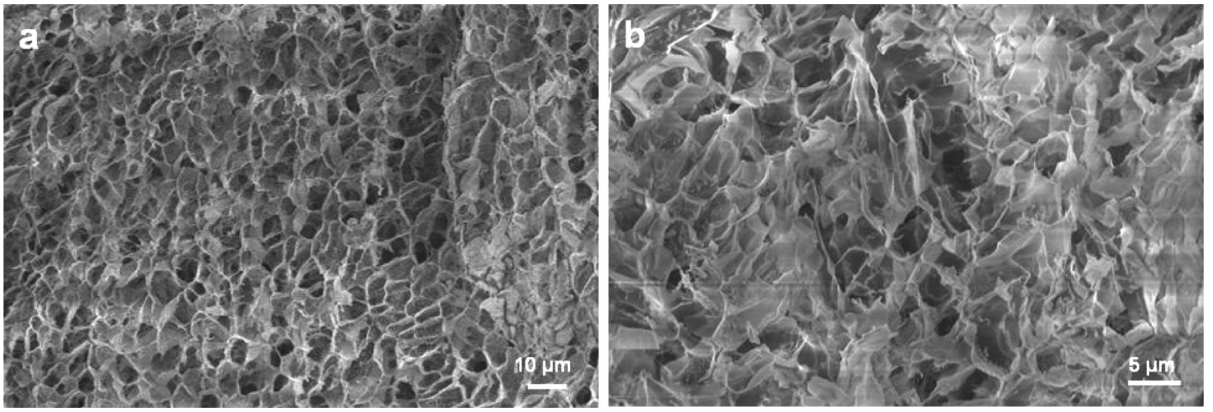

Figure 9. SEM images of freeze-dried (a) PAM and (b) 0.5 wt % graphene-PAM aerogels. Note that the graphene-PAM aerogels had a denser structure than the PAM aerogels.

increases. With only 0.5 wt % graphene loading, the chemically cross-linked graphene-PAM hydrogels and the physically cross-linked graphene-PAM hydrogels demonstrate 77% and 71% enhancements in toughness, respectively, compared to the chemically cross-linked baseline. This observation confirms that graphene sheets act as effective cross-linkers in the PAM hydrogels. In the absence of the chemical-cross-linker, the graphene sheets are postulated to aid in the process of energy dissipation and prevent crack-tip propagation.

It was also observed that the physically cross-linked graphene-PAM gels could be squeezed or freely bent (Figure 8a); in fact, these gels possess self-healing properties. As shown in Figure 8b, the hydrogel was cut into equal halves. These halves were then pushed together to create a surface contact and were heated at 70 °C in air for an hour. (No control experiment can be designed because graphene-free PAM samples do not gel.) The self-healed graphene-loaded hydrogels were swelled to equilibrium in distilled water without cracking (Supporting Information, Figure S7). This swelling experiment proves that the gels are truly self-healed, as the crack at the cut surface is completely repaired. (Note that the chemically cross-linked PAM hydrogels have chemical bonds present which are destroyed because of cutting and do not reform; hence, these PAM hydrogels do not exhibit self-healing.) A feasible mechanism for the self-healing of the physical hydrogels could be reversible adsorption. The polymer chains physisorb on graphene sheets, and the hydrogel self-heals via reformation of entanglements of the polymer chains at the cut surface. These re-entanglements are strong enough to withstand swelling forces.

Templates for Aerogels. The graphene-PAM hydrogels were freeze-dried after flash freezing in liquid nitrogen to yield low density graphene-PAM aerogels. The SEM images of the internal structure of the graphene-PAM (no cross-linker) and PAM aerogels are shown in Figure 9. However, the method of freeze-drying is destructive and alters the aerogel structure substantially compared to the original hydrogel. Even so, the pore diameter in the graphene-PAM aerogels was comparatively lower than that of the baseline PAM aerogel. This graphene-induced reduction in aerogel pore size correlates closely with the increased N^* caused by the presence of graphene in the hydrogels. The results suggest that the mesh size of the graphene gels may be smaller, assuming the aerogel pore size is related to mesh size in the precursor gel. This idea is consistent with the higher N^* in the graphene-loaded gels.

Figure 10 depicts the thermogravimetric analysis (TGA) of the freeze-dried aerogels. According to the TGA results, graphene-PAM hydrogels exhibit a higher thermal stability compared to the baseline PAM hydrogels. Around 110 °C the weight loss was assigned to the removal of residual water in the sample. The physically cross-linked graphene-PAM hydrogels exhibited the same degradation temperature as the chemically cross-linked graphene-PAM hydrogels. As graphene content increases in the PAM aerogels, the degradation temperature increases notably because of the high thermal conductivity of

dx.doi.org/10.1021/am402185r | ACS Appl. Mater. Interfaces 2013, 5, 8633−8640

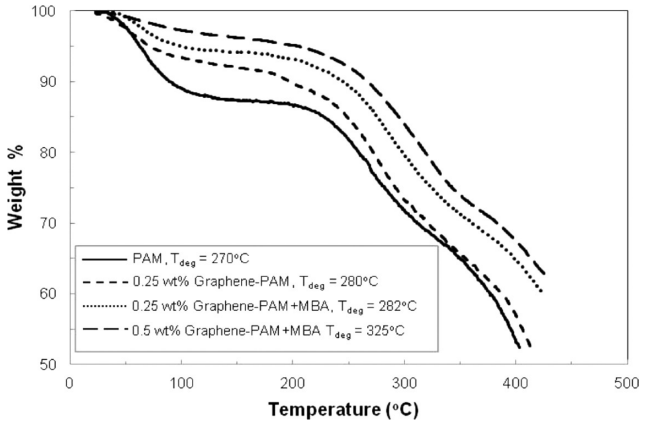

Figure 10. TGA curve for PAM, 0.25 wt % graphene-PAM, 0.25 wt % graphene-PAM+MBA, and 0.5 wt % graphene-PAM+MBA aerogels showing corresponding degradation temperatures. Addition of graphene as nanofiller significantly increases the thermal stability of the parent PAM aerogel.

graphene sheets and the restricted mobility of the polymer chains because of the presence of graphene.[53−55]

PAM aerogels with varying graphene-loadings (0.5, 1.5, and 2 wt % graphene) were synthesized using the same method. PAM is an insulator. It is observed that at 1.5 wt % graphene loading, the conductivity of the aerogel was 3.86×10^{-7} S/m (Table 1).

Table 1. Electrical Conductivity of Freeze-Dried Graphene-PAM Aerogels Shows Increasing Conductivity with Increasing Graphene Content

sample	conductivity, S/m
PAM	not conductive
0.5 wt % graphene-PAM	not conductive
1.5 wt % graphene-PAM	3.86×10^{-7}
2 wt % graphene-PAM	1.02×10^{-6}

With the increase of graphene loading to 2 wt %, the conductivity of the aerogel became 1.02×10^{-6} S/m. These conductivity values compare well against multiwalled carbon nanotube (MWNTs)/PAM composites, where conductivities of 3.48×10^{-8} S/m at 15 wt % MWNT and 0.012 S/m at 40 wt % MWNT were measured.[56]

4. CONCLUSION

On the basis of the experiments carried out, we propose a structure for the physically cross-linked graphene-PAM hydrogels. The exfoliated graphene sheets act as a successful multifunctional cross-linking agent for the polymer chains. The dispersion of the graphene sheets is uniform in the hydrogel matrix, and the presence of the PAM chains on the graphene surface aids in this dispersion. The polymer chains adhere to the graphene sheet surface, leading to an enhancement of the compressive properties of the hydrogel relative to the PAM analogue.

The experiments performed on these graphene-loaded hydrogels offer a clear picture of the structure and properties of the nanocomposite hydrogels. Novel pristine graphene and PAM hydrogels were successfully synthesized and characterized. Thus, the experiments performed on the graphene-loaded PAM system reveal that the presence of the nanofiller enhances the shear and compressive moduli of the hydrogel. Thus, it can be inferred that the PAM-stabilized graphene sheets interact well with the hydrogel without aggregation. The graphene sheets act as physical cross-link junctions, toughening the parent hydrogel, notably in the absence of a chemical cross-linker. We further explore the topic of percolation of nanofillers inside polymer aerogels and cryogels in another recent study.[57]

■ ASSOCIATED CONTENT

Supporting Information

Effects of molecular weight of PAM on final graphene concentration, absorbance spectra, additional TEM images, and effects of the monomer concentration on gel viscoelasticity. This material is available free of charge via the Internet at http://pubs.acs.org.

■ AUTHOR INFORMATION

Corresponding Author

*E-mail: micah.green@ttu.edu.

Notes

The authors declare no competing financial interest.

■ ACKNOWLEDGMENTS

We acknowledge the TTU Imaging Center (funded by NSF MRI 04-511) supported by Dr. Mark J. Grimson and Professor Lauren S. Gollahon for the SEM images. The authors would like to sincerely thank Francis Atore, Robert Fullerton, Shane Metzler, and Dorsa Parviz for helpful insights into the work. Funding was provided by the U.S. National Science Foundation (NSF) under CAREER award CMMI-1253085 and by the Air Force Office of Scientific Research Young Investigator Program (AFOSR FA9550-11-1-0027).

■ REFERENCES

(1) Peppas, N. A.; Bures, P.; Leobandung, W.; Ichikawa, H. *Eur. J. Pharm. Biopharm.* **2000**, *50* (1), 27−46.
(2) Peppas, N. A.; Hilt, J. Z.; Khademhosseini, A.; Langer, R. *Adv. Mater.* **2006**, *18* (11), 1345−1360.
(3) Qiu, Y.; Park, K. *Adv. Drug Delivery Rev.* **2001**, *53* (3), 321−339.
(4) Satarkar, N. S.; Biswal, D.; Hilt, J. Z. *Soft Matter* **2010**, *6* (11), 2364−2371.
(5) Gong, J. P.; Katsuyama, Y.; Kurokawa, T.; Osada, Y. *Adv. Mater.* **2003**, *15* (14), 1155−1158.
(6) Haque, M. A.; Kurokawa, T.; Gong, J. P. *Polymer* **2012**, *53* (9), 1805−1822.
(7) Sakai, T.; Matsunaga, T.; Yamamoto, Y.; Ito, C.; Yoshida, R.; Suzuki, S.; Sasaki, N.; Shibayama, M.; Chung, U.-i. *Macromolecules* **2008**, *41* (14), 5379−5384.
(8) Lin, W.-C.; Fan, W.; Marcellan, A.; Hourdet, D.; Creton, C. *Macromolecules* **2010**, *43* (5), 2554−2563.
(9) Haraguchi, K.; Takehisa, T.; Fan, S. *Macromolecules* **2002**, *35* (27), 10162−10171.
(10) Haraguchi, K.; Li, H. J.; Matsuda, K.; Takehisa, T.; Elliott, E. *Macromolecules* **2005**, *38* (8), 3482−3490.
(11) Haraguchi, K. *Curr. Opin. Solid State Mater. Sci.* **2007**, *11* (3−4), 47−54.
(12) Haraguchi, K.; Farnworth, R.; Ohbayashi, A.; Takehisa, T. *Macromolecules* **2003**, *36* (15), 5732−5741.
(13) Xiong, L.; Hu, X.; Liu, X.; Tong, Z. *Polymer* **2008**, *49* (23), 5064−5071.
(14) Zhang, Q.; Li, X.; Zhao, Y.; Chen, L. *Appl. Clay Sci.* **2009**, *46* (4), 346−350.
(15) Geim, A. K.; Novoselov, K. S. *Nat. Mater.* **2007**, *6* (3), 183−191.
(16) Novoselov, K. S.; Jiang, D.; Schedin, F.; Booth, T. J.; Khotkevich, V. V.; Morozov, S. V.; Geim, A. K. *Proc. Natl. Acad. Sci. U.S.A.* **2005**, *102* (30), 10451−10453.

(17) Obraztsov, A. N. *Nat. Nanotechnol.* **2009**, *4* (4), 212−213.
(18) Lotya, M.; Hernandez, Y.; King, P. J.; Smith, R. J.; Nicolosi, V.; Karlsson, L. S.; Blighe, F. M.; De, S.; Wang, Z. M.; McGovern, I. T.; Duesberg, G. S.; Coleman, J. N. *J. Am. Chem. Soc.* **2009**, *131* (10), 3611−3620.
(19) Stankovich, S.; Dikin, D. A.; Piner, R. D.; Kohlhaas, K. A.; Kleinhammes, A.; Jia, Y.; Wu, Y.; Nguyen, S. T.; Ruoff, R. S. *Carbon* **2007**, *45* (7), 1558−1565.
(20) McAllister, M. J.; Li, J. L.; Adamson, D. H.; Schniepp, H. C.; Abdala, A. A.; Liu, J.; Herrera-Alonso, M.; Milius, D. L.; Car, R.; Prud'homme, R. K.; Aksay, I. A. *Chem. Mater.* **2007**, *19* (18), 4396−4404.
(21) Gomez-Navarro, C.; Weitz, R. T.; Bittner, A. M.; Scolari, M.; Mews, A.; Burghard, M.; Kern, K. *Nano Lett.* **2007**, *7* (11), 3499−3503.
(22) Rourke, J. P.; Pandey, P. A.; Moore, J. J.; Bates, M.; Kinloch, I. A.; Young, R. J.; Wilson, N. R. *Angew. Chem., Int. Ed.* **2011**, *50* (14), 3173−3177.
(23) Bourlinos, A. B.; Georgakilas, V.; Zboril, R.; Steriotis, T. A.; Stubos, A. K.; Trapalis, C. *Solid State Commun.* **2009**, *149* (47−48), 2172−2176.
(24) Green, A. A.; Hersam, M. C. *Nano Lett.* **2009**, *9* (12), 4031−4036.
(25) Parviz, D.; Das, S.; Ahmed, H. S. T.; Irin, F.; Bhattacharia, S.; Green, M. J. *ACS Nano* **2012**, *6* (10), 8857−8867.
(26) Wajid, A. S.; Ahmed, H. S. T.; Das, S.; Irin, F.; Jankowski, A. F.; Green, M. J. *Macromol. Mater. Eng.* **2013**, *298*, 339−347.
(27) Wajid, A. S.; Das, S.; Irin, F.; Ahmed, H. S. T.; Shelburne, J. L.; Parviz, D.; Fullerton, R. J.; Jankowski, A. F.; Hedden, R. C.; Green, M. J. *Carbon* **2012**, *50*, 526−534.
(28) Das, S.; Irin, F.; Ahmed, H. S. T.; Cortinas, A. B.; Wajid, A. S.; Parviz, D.; Jankowski, A. F.; Kato, M.; Green, M. J. *Polymer* **2012**, *53* (12), 2485−2494.
(29) Lotya, M.; King, P. J.; Khan, U.; De, S.; Coleman, J. N. *ACS Nano* **2010**, *4* (6), 3155−3162.
(30) Liu, R.; Liang, S.; Tang, X.-Z.; Yan, D.; Li, X.; Yu, Z.-Z. *J. Mater. Chem.* **2012**, *22* (28), 14160−14167.
(31) Xu, Y. X.; Wu, Q. O.; Sun, Y. Q.; Bai, H.; Shi, G. Q. *ACS Nano* **2010**, *4* (12), 7358−7362.
(32) Liu, J. Q.; Chen, C. F.; He, C. C.; Zhao, L.; Yang, X. J.; Wang, H. L. *ACS Nano* **2012**, *6* (9), 8194−8202.
(33) Liu, J.; Song, G.; He, C.; Wang, H. *Macromol. Rapid Commun.* **2013**, *34* (12), 1002−1007.
(34) Shen, J.; Yan, B.; Li, T.; Long, Y.; Li, N.; Ye, M. *Composites, Part A* **2012**, *43* (9), 1476−1481.
(35) Adhikari, B.; Biswas, A.; Banerjee, A. *Langmuir* **2012**, *28* (2), 1460−1469.
(36) Bai, H.; Sheng, K.; Zhang, P.; Li, C.; Shi, G. *J. Mater. Chem.* **2011**, *21* (46), 18653−18658.
(37) Bai, H.; Li, C.; Wang, X. L.; Shi, G. Q. *Chem. Commun.* **2010**, *46* (14), 2376−2378.
(38) Xu, Y. X.; Sheng, K. X.; Li, C.; Shi, G. Q. *ACS Nano* **2010**, *4* (7), 4324−4330.
(39) Worsley, M. A.; Pauzauskie, P. J.; Olson, T. Y.; Biener, J.; Satcher, J. H.; Baumann, T. F. *J. Am. Chem. Soc.* **2010**, *132* (40), 14067−14069.
(40) Ren, L. L.; Liu, T. X.; Guo, J. A.; Guo, S. Z.; Wang, X. Y.; Wang, W. Z. *Nanotechnology* **2010**, *21* (33), 7.
(41) Fan, J.; Shi, Z.; Wang, J.; Yin, J. *Polymer* **2013**, *54* (15), 3921−3930.
(42) Yavari-Gohar, M. R.; Kabiri, K.; Zohuriaan-Mehr, M. J.; Hashemi, S. A. *J. Polym. Res.* **2010**, *17* (2), 151−159.
(43) Shi, J. H.; Guo, Z. X.; Zhan, B. H.; Luo, H. X.; Li, Y. F.; Zhu, D. B. *J. Phys. Chem. B* **2005**, *109* (31), 14789−14791.
(44) Manley, S.; Davidovitch, B.; Davies, N. R.; Cipelletti, L.; Bailey, A. E.; Christianson, R. J.; Gasser, U.; Prasad, V.; Segre, P. N.; Doherty, M. P.; Sankaran, S.; Jankovsky, A. L.; Shiley, B.; Bowen, J.; Eggers, J.; Kurta, C.; Lorik, T.; Weitz, D. A. *Phys. Rev. Lett.* **2005**, *95* (4), 048302.
(45) Okay, O.; Oppermann, W. *Macromolecules* **2007**, *40* (9), 3378−3387.
(46) Agrawal, S. K.; Sanabria-DeLong, N.; Tew, G. N.; Bhatia, S. R. *Langmuir* **2010**, *26* (14), 12472−12472.
(47) Zhou, C.; Wu, Q.; Zhang, Q. *Colloid Polym. Sci.* **2011**, *289* (3), 247−255.
(48) Wu, L.; Zeng, L.; Chen, H.; Zhang, C. *Polym. Bull.* **2012**, *68* (2), 309−316.
(49) Bhattacharyya, S.; Guillott, S.; Dabboue, H.; Tranchant, J.-F.; Salvetat, J.-P. *Biomacromolecules* **2008**, *9* (2), 505−509.
(50) Samanta, S. K.; Pal, A.; Bhattacharya, S.; Rao, C. N. R. *J. Mater. Chem.* **2010**, *20* (33), 6881−6890.
(51) Wang, J.; Ugaz, V. M. *Electrophoresis* **2006**, *27* (17), 3349−3358.
(52) Tong, X.; Zheng, J.; Lu, Y.; Zhang, Z.; Cheng, H. *Mater. Lett.* **2007**, *61* (8−9), 1704−1706.
(53) Balandin, A. A.; Ghosh, S.; Bao, W.; Calizo, I.; Teweldebrhan, D.; Miao, F.; Lau, C. N. *Nano Lett.* **2008**, *8* (3), 902−907.
(54) Yang, X.; Shang, S.; Li, L. *J. Appl. Polym. Sci.* **2011**, *120* (3), 1355−1360.
(55) Jiang, L.; Shen, X.-P.; Wu, J.-L.; Shen, K.-C. *J. Appl. Polym. Sci.* **2010**, *118* (1), 275−279.
(56) Awasthi, K.; Kumar, R.; Raghubanshi, H.; Awasthi, S.; Pandey, R.; Singh, D.; Yadav, T. P.; Srivastava, O. N. *Bull. Mater. Sci.* **2011**, *34* (4), 607−614.
(57) Irin, F.; Das, S.; Atore, F. O.; Green, M. J. *Langmuir* **2013**, DOI: 10.1021/la4017307.